Hearing Research 387 (2020) 107861

Contents lists available at ScienceDirect

Hearing Research

journal homepage: www.elsevier.com/locate/heares

Research Paper

# Active tympanic tuning facilitates sound localization in animals with internally coupled ears

Anupam P. Vedurmudi [a, 1], Bruce A. Young [b, 1], J. Leo van Hemmen [c, *]

[a] Forschungs-Neutronenquelle Heinz Maier-Leibnitz, Technische Universität München, 85748, Garching bei München, Germany
[b] Kirksville College of Osteopathic Medicine, A.T. Still University, Kirksville, MO, 63501, USA
[c] Physik Department, Technische Universität München, 85747, Garching bei München, Germany

ARTICLE INFO

*Article history:*
Received 19 July 2019
Received in revised form
12 November 2019
Accepted 2 December 2019
Available online 19 December 2019

*Keywords:*
Tympanic membrane
Skeletal muscle
Tension
Fundamental frequency
Internally coupled ears
Auditory perception
Sound localization

ABSTRACT

Earlier studies have reported that numerous vertebrate taxa have skeletal muscle(s) attaching directly, or indirectly, onto the tympanic membrane. The present study links these prior studies by quantitatively modeling the influence of skeletal muscle contraction on tympanic tension, tympanic dampening, and, ultimately, the fundamental frequency. In this way, the efficacy of these tympanic muscles to dynamically alter the sensory response of the vertebrate ear is quantified. Changing the tension modifies the eardrum's fundamental frequency, a key notion in understanding hearing through internally coupled ears (ICE) as used by the majority of terrestrial vertebrates. Tympanic tension can also be modulated by altering the pressure acting on the deep (medial) surface of the tympanum. Herein we use the monitor lizard *Varanus* as an example to demonstrate how active modulation of the pharyngeal volume permits tuning of an ICE auditory system. The present contribution offers a behaviorally and biologically realistic perspective on the ICE system, by demonstrating how an organism can dynamically alter its morphology to tune the auditory response. Through quantification of the relationships between tympanic surface tension, damping, membrane fundamental frequency, and auditory cavity volume, it can be shown that an ICE system affords a biologically relevant range of tuning.



## 1. Introduction: Tuning auditory perception

A tympanum, or eardrum, functions as a drum under tension, and many taxa can regulate the tension of their tympanum. Herein the ability of vertebrates to actively tune the tympanum will be modeled with particular reference to monitor lizards (*Varanus*); see Fig. 1. As will be shown, their system of internally coupled ears (hereafter ICE) plays a key role since the two tympana are linked internally by relatively large, air-filled passageways. Our analysis applies equally to other taxa with ICE. In most vertebrates the tympanic membrane is anchored to skeletal muscle for a portion of the membrane's margin, and the tympanum itself, or the coupled extracolumella, can be a site of skeletal muscle attachment (Wever, 1978; Young, 2016). As Fig. 1b demonstrates, in *Varanus* the junction between the tympanic membrane and the adjacent skeletal muscle (the depressor mandibulae) gives rise to a block of connective tissue (the post-tympanic band), which includes elastic fibers that integrate into the tympanum, as well as a skeletal muscle (the tympanus) that inserts onto the distal ends of the extracolumella and is integrated into the tympanum (Han and Young, 2016).

The majority of non-mammalian terrestrial vertebrates have ICE (see van Hemmen et al. (2016)). With this anatomical linkage, deflection of one tympanic membrane creates an internal pressure wave that propagates through the air-filled passageway to drive the contralateral tympanic membrane (Christensen-Dalsgaard and Manley, 2005, 2008; Vossen et al., 2010; van Hemmen et al., 2016). A recent biophysical model of the ICE system (Vedurmudi et al., 2016a, b) has demonstrated that ICE resulted in both temporal (termed internal Time Difference, or iTD) and amplitude (termed internal Level Difference, or iLD) cues, and that the magnitude of these cues was directionally determined (Vedurmudi et al., 2016a, b). All predictions are nicely compatible with experiment (Christensen-Dalsgaard and Manley, 2008). It is important to realize that what the animal hears is *not* the externally perceived interaural time and level difference stimuli (the ITD and ILD), but

* Corresponding author.
*E-mail addresses:* anupam.vedurmudi@tum.de (A.P. Vedurmudi), byoung@atsu.edu (B.A. Young), lvh@tum.de (J.L. van Hemmen).
[1] Contributed equally.

https://doi.org/10.1016/j.heares.2019.107861

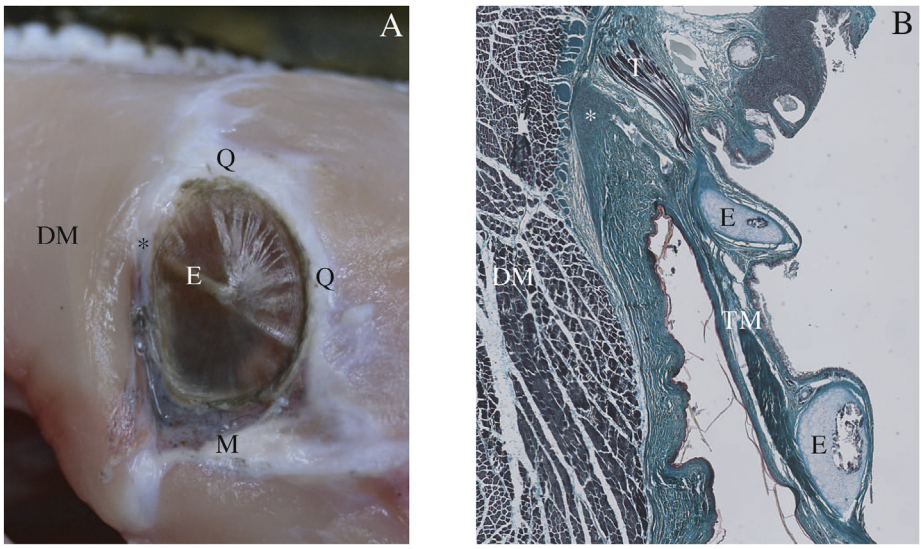


(a) *Varanid* tympanic membrane (b) Histological section

**Fig. 1.** The tympanic membrane (A) of *Varanus* attaches caudally to a thick band of connective tissue (*) located on the cranial surface of the depressor mandibulae muscle. A histological section at this level (B) reveals the tympanus muscle extending from the surface of the depressor mandibulae and inserting onto the extracolumella as well as integrating into the tympanic membrane; contraction of the tympanus can exert radial tension on the tympanic membrane. Abbreviations: DM – depressor mandibulae, E – extracolumella, Q – quadrate, M – mandible, **T** – tympanus, TM – tympanic membrane.

rather the internal ones (the iTD and iLD) that result from the simultaneous interaction of the external stimuli and the internally coupled tympana.

There are complex tension profiles over the tympanic membrane of *Varanus* (Han and Young, 2018); the skeletal muscles around the tympanum suggest that *Varanus* can actively change both the axial and radial tensions acting on the tympanum. We will analyze how changes to the fundamental frequency and dampening of the tympanum produce shifts in the frequency response of the internally coupled ears.

In many vertebrates with ICE a portion of the air-filled passageway linking the contralateral ears is formed by the pharyngeal cavity; see Fig. 2. Monitor lizards, and many other reptiles, can voluntarily expand their pharyngeal space ventrally forming a gular pouch. Expansion of the gular is used as a visual display for both inter- and intra-specific encounters (Murphy and Mitchell, 1974; Murphy and Lamoreaux, 1978), and it can also be used as an additional means of ventilator airflow (Owerkowicz et al., 1999). The size of the gular region, and thus the pharyngeal cavity as a whole, is under active control involving skeletal muscles of the hyoid complex (Owerkowicz et al., 2001). Here we demonstrate how changes to the volume of the anatomical coupling between the tympana produce shifts in the frequency response of internally coupled ears.

*Synopsis.* In section 2 we model the eardrum mathematically and analyze its boundary conditions and frequency response, including the excess gular pressure $\Delta P$ and the tympanus muscle exerting an additional tension $\mathscr{T}_{\text{app}}$. In so doing we will also account for the membrane's Poisson ratio $\nu_M$. As the wavelengths relevant to the animal are typically $<2$ kHz and, hence, have wavelengths $\lambda < 15$ cm, we can safely restrict our attention to cylinders as cavity shapes. In lizards, the cross-section of the pharyngeal "cylinder" may well be wider than the tympana (Fig. 6). In section 3 we allow for a variation of the inner cavity with respect to the cylinder spanned by the eardrum. Section 4 is devoted to the auditory cues proper, the internal time and level difference, iTD & iLD. Because the eardrum's fundamental frequency $f_0$ segregates the iTD and iLD regimes, tuning $f_0$ directly modifies auditory

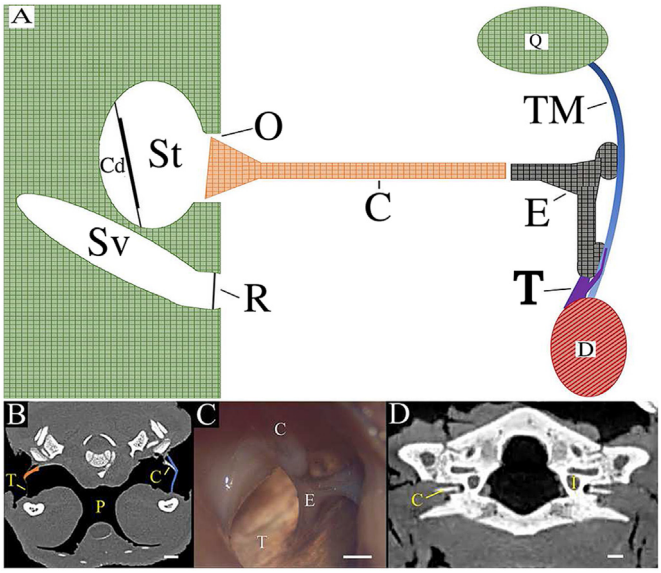


**Fig. 2.** The Anatomy of the auditory system in Varanus. A) Generalized schematic of a horizontal section through the ear, Sound-conducting system of *Varanus*. B) micro-CT scan showing the prominent interaural canal linking the two tympana (T, and red contralateral) and incorporating the pharyngeal cavity (P); the extracolumella/columella (C, and blue contralateral) is visible on the medial surface of the tympanum. C) Dissection of the middle ear showing the junction between the columella (C) and extracolumella (E), and the integration between the extracolumella and the tympanic membrane (T). D) Magnified slice of a micro-CT scan showing the proximal end of the columella (C) expanding as the footplate within the oval window, on the lateral margin of the inner ear cavity (I). Note that despite the columella being perpendicular to the tympanum it is difficult to capture the full length of the columella in a single image. This is due to the expanded distal end of the extracolumella (evident in B), the high mobility of the quadrate (which shifts the distal end of the columella relative to the proximal end), and the thin slices used in present imaging techniques. Abbreviations: C – columella; Cd – cochlear duct; D – depressor mandibulae; E – extracolumella; I – inner ear; M – middle ear cavity; O – oval window; P – pharynx; Q – quadrate; R – round window; St – scala tympana; SV – scala vestibula; TM – tympanic membrane; T – tympanus muscle. Scale bars – B: 5 mm, C: 1 mm, D: 1 mm. (For interpretation of the references to color in this figure legend, the reader is referred to the Web version of this article.)

processing. A discussion of various interpretations and spin-offs concludes the paper. The Appendix details why we have modeled the tympanum as a drum whose dynamical response is governed by tension, rather than as a pre-curved dome with a bending-dominated response as Fig. 1a seems to suggest. The appendix also provides a dimensional analysis.

## 2. Vibration of the eardrums

The dynamics of the tympanic membrane is determined by its fundamental frequency $f_0$ and its inherent damping, which we quantify by means of a damping coefficient $\alpha$ to be specified below. The tympanic membrane is modeled as a circular membrane clamped at its boundaries with an attached sectorial plate representing the extracolumella at the circumference. The extracolumella serves as a transducer for the membrane vibrations, which are transmitted through the columella to the inner ear. However, the extracolumella is effectively of infinite mass and motionless, a reasonable approximation since the extracolumella and attached proximal elements are typically much (300 × ) heavier than the rest of the membrane.

Given the large mass of the extracolumella and the attached middle-ear bone, we have therefore neglected the motion of the extracolumella in solving the dynamics of the eardrum in response to external sound. The motion of the eardrum can then be used to calculate the forces acting on the cochlea using the exact mass of the system of extracolumella + columella.

Consequently and as shown schematically by Fig. 3b, a reptilian eardrum is safely modeled as a thin, circular, and linear-elastic membrane of radius $a_{\text{tymp}}$ that is asymmetrically loaded by an extracolumella Vedurmudi et al. (2016a, b), such that the vibrating part of its surface is limited to

$$S_{\text{mem}} = (r, \phi) \in (0, a_{\text{tymp}}) \times (\beta, 2\pi - \beta) \tag{1}$$

where the wedge $(-\beta, \beta)$ has been taken out to represent the extracolumella and $\beta$ is at our disposal as a parameter reflecting the situation at hand. The displacement $u(r, \phi; t)$ of an eardrum driven by an external pressure $p^{\text{ex}}$ and an internal pressure $p^{\text{in}}$ is given by a damped two-dimensional wave equation

$$-\frac{\partial^2 u^{0/L}}{\partial t^2} - 2\alpha \frac{\partial u^{0/L}}{\partial t} + c_M^2 \Delta_{(2)} u^{0/L} = \frac{p^{\text{ex}}_{0/L} - p^{\text{in}}_{0/L}}{\rho_M d_M} \tag{2}$$

where $\rho_M$ is the density of the membrane and $d_M$ is its thickness. The two-dimensional Laplacian (henceforth given in polar coordinates) is denoted by $\Delta_{(2)}$. For $\alpha = 0$, the propagation speed of waves on the membrane surface $c_M$ is related to the membrane tension $T$ by (Kreyszig, 2010, p. 577, p. 577)

$$c_M = \sqrt{T/\rho_M d_M}\,. \tag{3}$$

The external component of the driving pressure $p^{\text{ex}}$ is generated by an external sound source, while the internal pressure $p^{\text{in}}$ arises due to the interaction of the eardrum with the air inside the interaural cavity. Both will be discussed thoroughly in subsequent sections.

Given a uniform, pure-tone uniform driving pressure of the form $p(r, \phi; t) = pe^{i\omega t}$, the quasi-steady-state solution to Eq. (2) for a frequency $f$ (angular frequency $\omega = 2\pi f$) is given by an expansion in terms of an infinite set of orthogonal modes $u_{mn}$

$$u^{0/L}(r, \phi; t) = \sum_{m,n}^{\infty} C^{0/L}_{mn} u_{mn}(r, \phi) e^{i\omega t} \tag{4}$$

where $u_{mn}(r, \phi) = \sin\kappa(\phi - \beta) J_\kappa(\mu_{mn} r)$ and $\mu_{mn} \times a_{\text{tymp}}$ is the $n^{\text{th}}$ zero of the order-$\kappa$ Bessel function $J_\kappa$ of the first kind, such that $\kappa = m\pi/2(\pi - \beta)$ with $m \in \mathbb{N}$ a positive integer. The $u_{mn}$ correspond to the eigenmodes of the Laplacian $\Delta_{(2)}$ on a sectorial disk − see Fig. 3b − with Dirichlet boundary conditions in Eq. (2).

The operater $-\Delta_{(2)}$, which is minus the Laplacian, is positive-definite and its lowest eigenvalue is related to the fundamental frequency $f_0$ of the membrane through

$$f_0 = \frac{c_M \mu_{11}}{2\pi} = \frac{\mu_{11}}{2\pi} \sqrt{T/\rho_M d_M}\,, \tag{5}$$

where $c_M$ is the propagation speed of waves on the membrane surface and $T$ is the membrane tension.

### 2.1. Eardrum's frequency response

For our subsequent calculations, it is convenient to define a tympanic frequency response $\Lambda$ that gives us its integral steady-state displacement for a uniform, pure-tone, input. Proceeding from Eq. (2) and using the membrane eigenmodes $u_{mn}$ defined previously, we find that the integral displacement or "volume velocity" $S$ of a single tympanic membrane driven by a *uniform* pressure $p \exp(i\omega t)$ takes the form

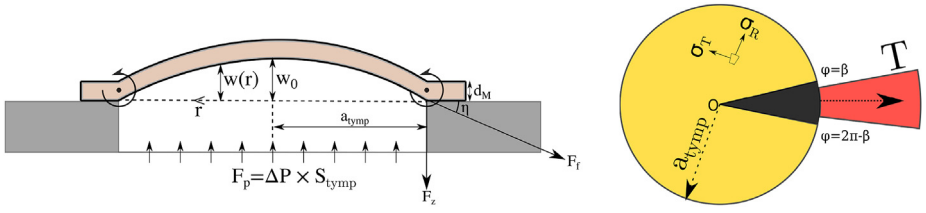


(a) Membrane deformation (b) Eardrum surface

**Fig. 3.** (Color online) (a) Membrane deformation under pressure difference $\Delta P$, which is the *static* difference between the external atmospheric and internal pressure because of gular ventilation. For small values of $\Delta P$, the deflection is modeled as a parabola $w(r)$ with a maximum deflection $w_0$ at the center. The pressure difference results in a net force of $\Delta P \times S_{\text{tymp}}$ acting on the eardrum of area $S_{\text{tymp}}$. In response to its deformation the membrane tension applies a force $F_f$ at its circumference, such that its normal component $F_z$ compensates for the force due to $\Delta P$. The dot and arrow on either side indicate that, due to the lizard-specific biophysics of attachment, the membrane boundary allows free rotations; see also the Appendix. Figure adapted from Schomburg (2015). (b) View of the surface of the model eardrum for *Varanus*. The black sector between $\phi = 2\pi - \beta$ and $\phi = \beta$ corresponds to the non-moving surface of the extracolumella, while the remaining portion corresponds to the vibrating surface of the eardrum. For the mechanics of transduction of sound from the extracolumella (black) via the columella to the cochlea, see Manley (1990, particularly Fig. 3.8). The directions of the forces acting on an element of the eardrum due to the radial and axial stresses are indicated by the arrows and $\sigma_{R/T}$, as is the tympanus muscle (T) in red with the arrow indicating the direction of the force applied by the muscle. (For interpretation of the references to color in this figure legend, the reader is referred to the Web version of this article.)

$$S = \int_{S_{\text{mem}}} dS\, u(r,\phi;t) = \Lambda(\omega)\, p\, e^{i\omega t} \tag{6}$$

where

$$\Lambda(\omega) = \sum_{m,n\geq 1}^{\infty} \frac{\left(\int dS\, u_{mn}\right)^2}{\Omega_{mn}\int dS\, u_{mn}^2} \tag{7}$$

and

$$\Omega_{mn} = \rho_M d_M \left(\omega^2 - 2i\alpha\omega - c_M^2\mu_{mn}^2\right) \quad m,n \geq 1\,. \tag{8}$$

Finally, we also define the damping ratio $\zeta$ as the ratio between the damping coefficient $\alpha$ and the angular fundamental frequency $\omega_0 = 2\pi f_0$,

$$\zeta = \alpha/\omega_0\,. \tag{9}$$

The use of $\Lambda(\omega)$ will simplify our calculations for the vibration of the coupled membranes.

### 2.2. Tuning the eardrum

In *Varanus*, the eardrum tension $T$ and, as a result, its fundamental frequency can be varied both by means of.

- a pressure difference across its surface via gular inflation,
- radial stretching using the tympanus muscle.

In the present subsection, we discuss the influence of both these mechanisms on the eardrum tension. For the sake of clarity, we limit our discussion to the behavior of a fully circular membrane with an initial uniform tension $T$ for the animal in its "relaxed" state. In both cases, we aim to find expressions for the resulting increase in tension $\Delta T$.

*Gular inflation.*

The ventilation (or evacuation) of the gular results in an outward (or inward) displacement of the membrane surface and, consequently, a change in its tension. The deformation $w$ of the membrane from its equilibrium position, subject to a uniform *static* pressure difference $\Delta P$, can be obtained as a solution to the static version ($\partial u/\partial t, \partial^2 u/\partial^2 t \to 0$) of the membrane equation (2)

$$\tilde{c}_M \Delta_{(2)} w = \Delta P\,/\,\rho_M d_M\,. \tag{10}$$

The wave speed is now given by $\tilde{c}_M = \sqrt{(T+\Delta T)/\rho_M d_M}$, as the deformation of the membrane results in an increased tension $T + \Delta T$; cf. Eq. (3). Note that the static pressure $\Delta P$ is distinct from the internal and external sound pressures $p^{\text{in/ex}}$ on the eardrum surface, which will be defined later.

In contrast to the excitation of the eardrum surface by means of sound pressure (2), the pressure increase because of gular expansion is significantly higher than typical sound pressures [98 Pa (1 cm $H_2O$) as opposed to 20 mPa at 60 dB SPL] and is constant in time, i.e., of frequency zero. Consequently, it is also no longer accurate to assume that the extracolumella remains stationary. That is, the center O of the membrane-extracolumella system (see Fig. 3b) is also pushed outwards and a purely radial version Eq. (10) is a reasonable model for the surface of the deformed eardrum. Equation (2) in contrast models the dynamics of the eardrum for a "resting" tension that is now higher or lower according to the gular pressure.

For small values of $\Delta P$, the purely radial version of Eq. (10) can be solved by imposing a Dirichlet condition at its outer boundary ($r = a_{\text{tymp}}$) and requiring the finiteness of $w(r)$ at $r = 0$. The thin *circular* membrane now adopts a parabolic shape and its deflection $w(r)$ is given by the equation (Timoshenko and Woinowsky-Krieger, 1959)

$$w(r) = w_0\left(1 - \frac{r^2}{a_{\text{tymp}}^2}\right), \tag{11}$$

$$w_0 = \Delta P a_{\text{tymp}}^2 \,\Big/\, (T + \Delta T)\,, \tag{12}$$

where $a_{\text{tymp}}$ is the radius of the membrane, $r$ is the distance from the center and $w_0$ is the height of the deformation at the center.

Alternatively (Schomburg, 2015), the net vertical force on the membrane surface due to a *static* pressure difference $F_p = \Delta P \pi a_{\text{tymp}}^2$ is balanced by the vertical component of the force exerted by the frame fixing the membrane at its circumference $F_z = F_f \sin\eta$, where $\eta$ is the angle between the tangent to the membrane surface and the horizontal at the membrane boundary; cf. Fig. 3a. The force $F_f$ exerted by the frame is equal and opposite to the force exerted by the membrane on the frame due to its increased tension $T + \Delta T$. For small values of the angle $\eta$ we have $\sin\eta \approx \tan\eta$, which gives us

$$F_p = \Delta P(\pi - \beta) a_{\text{tymp}}^2 = -F_z = -\underbrace{(T+\Delta T) 2\pi a_{\text{tymp}}}_{=F_f} \tan\eta\,. \tag{13}$$

Substituting

$$\tan\eta = \left.\frac{dw}{dr}\right|_{r=a_{\text{tymp}}} = -2w_0 r \,\Big/\, a_{\text{tymp}}$$

into the above equation (13) returns the expression given in Eq. (12)

Subsequently to the application of a pressure difference, the resulting stress $\sigma_M$ in the deflected membrane is given by

$$\sigma_M = \sigma_0 + \sigma_D \tag{14}$$

where

$$\sigma_0 = T/d_M \quad \text{and} \quad \sigma_D = \Delta T/d_M \tag{15}$$

are the residual stress already present before deformation and the additional stress generated due to the deflection, respectively. The latter can be calculated from the radial ($\sigma_R$) and tangential ($\sigma_T$) components of the stress (cf. Fig. 3b) and can be written in terms of Young's modulus $E_M$ and Poisson ratio $\nu_M$ of the eardrum,

$$\varepsilon_R = \frac{\sigma_R}{E_M} + \nu_M \frac{\sigma_T}{E_M}\,, \quad \varepsilon_T = \frac{\sigma_T}{E_M} + \nu_M \frac{\sigma_R}{E_M}\,. \tag{16}$$

The radial strain is given by the relative change in the diameter of the membrane, which can be calculated from the length of the resulting parabola [see (11)]

$$L_p \approx 2a_{\text{tymp}}\left[1 + \frac{2}{3}\left(\frac{w_0}{a_{\text{tymp}}}\right)^2 + \mathscr{O}\left(\left(\frac{w_0}{R_M}\right)^4\right)\right], \tag{17}$$

$$\Rightarrow \varepsilon_R = -1 + L_p \,\Big/\, 2a_{\text{tymp}} \approx \frac{2}{3}\left(\frac{w_0}{a_{\text{tymp}}}\right)^2. \tag{18}$$

Since the membrane is clamped at its boundary, where it can effectively rotate freely, and the pressure difference $\Delta P$ is applied uniformly over its surface, we may assume that the tangential strain $\varepsilon_T$ is zero everywhere, resulting in the following radial stress-strain relation,

$$\sigma_D = \sigma_R = \varepsilon_R \frac{E_M}{1-\nu_M^2} \,. \tag{19}$$

Using the above equation along with the expression for the radial strain (18) the membrane stress $\sigma_M$ can be written

$$\sigma_M = \sigma_0 + \frac{2}{3}\frac{w_0^2}{a_{\text{tymp}}^2}\frac{E_M}{1-\nu_M^2} \,. \tag{20}$$

The above equation, along with the expressions for $\sigma_{M/0}$ in terms of the membrane tension (15), can now be used to eliminate $w_0$ from (12),

$$\Delta P = 2\sqrt{6(1-\nu_M^2)\frac{\sigma_M-\sigma_0}{E_M}}\,\frac{d_M}{a_{\text{tymp}}}\sigma_M \tag{21}$$

$$= 2\sqrt{6(1-\nu_M^2)\frac{\Delta T}{E_M d_M}}\,\frac{(T+\Delta T)}{a_{\text{tymp}}} \,, \tag{22}$$

which, upon squaring, results in a cubic equation in $\Delta T$,

$$\frac{\Delta T^3}{T^3} + 2\frac{\Delta T^2}{T^2} + \frac{\Delta T}{T} - b = 0 \tag{23}$$

where

$$b = \frac{E_M d_M a_{\text{tymp}}^2 \Delta P^2}{24(1-\nu_M^2)T^3} \,. \tag{24}$$

As the discriminant of the cubic equation (23) is always negative, it has one real and two complex conjugate roots (Irving, 2004).

Fig. 4a shows the relative change in the fundamental frequency $\Delta f_0/f_0$ against the change in gular pressure $\Delta P$, as calculated from the tension using Eq. (5). Here $\Delta P$ is chosen by the animal, which is then kept fixed. The quadratic dependence of $\Delta T$ on small values of $\Delta P$ (23) is reflected in the symmetry of the curve around $\Delta P = 0$. Moreover, for smaller $\Delta P$ or, more precisely, smaller values of $b$ as defined in Eq. (24), the variation in $\Delta f_0$ does not depend strongly on the Poisson ratio $\nu_M$. For very large values of $\Delta P$, the dependence upon $\nu_M$ becomes apparent in that larger values of $\nu_M$ result in greater increases in $f_0$. Fig. 4b exhibits the relative variation of the damping ratio $\zeta$ defined in Eq. (9) in dependence upon the gular pressure. As the damping coefficient $\alpha$ remains constant, we see a decrease in $\zeta$ with increasing membrane tension $T$.

*Using the tympanus muscle*

The effect of the tympanus muscle on the eardrum is modeled as a uniform radial stretching of the membrane. Though the action of the tympanus muscle on the membrane is nonuniform (cf. Fig. 3b), the position of its attachment effectively results in a pulling of the extracolumella; see Fig. 1. Accordingly, we emulate its effect by a uniform increase in tension. The relation between the membrane stresses $\sigma_{M/0}$ and the membrane tension $T$ remain the same as in Eq. (15), as do the Hookean and, hence, linear stress-strain relations (16). On the other hand, the radial strain due to the deformation, which is equivalent to the relative change in the membrane radius, is now given by

$$\varepsilon_R = -1 + (a_{\text{tymp}} + \Delta r)\,/\,a_{\text{tymp}} \approx \Delta r\,/\,a_{\text{tymp}} \tag{25}$$

The above expression for the radial strain can be used to compute the deformation stress in terms of $E_M$ and $\nu_M$. Moreover, as the tension applied by the tympanus muscle only acts on its outer periphery, the presence of the extracolumella is not relevant to the present discussion as in the case of gular expansion (12). The resulting membrane stress $\sigma_M$ is related to the initial stress $\sigma_0$ by

$$\sigma_M = \sigma_0 + \varepsilon_R \frac{E_M}{1-\nu_M^2} \tag{26}$$

where, as in Eq. (19), we have assumed that the tangential strain $\varepsilon_T$ vanishes. Denoting the applied tension by $\mathscr{T}_{\text{app}}$, we can relate the change in tension $\Delta T$ to the membrane stresses $\sigma_{0/M}$ via (15) by means of the expression

$$\mathscr{T}_{\text{app}} = \Delta T = d_M(\sigma_M - \sigma_0) \,. \tag{27}$$

The above equation can be used in conjunction with Eq. (5) to derive an expression for the change in fundamental frequency $\Delta f_0$ in terms of $\mathscr{T}_{\text{app}}$ and the increased tympanic radius $a_{\text{tymp}}(1+\varepsilon_R)$

$$\Delta f_0 = \frac{\mu_{11}}{2\pi(1+\varepsilon_R)}\sqrt{\frac{T+\mathscr{T}_{\text{app}}}{\rho_M d_M}} - f_0 \tag{28}$$

where

$$\varepsilon_R = \frac{\mathscr{T}_{\text{app}}(1-\nu_M^2)}{d_M E_M} \,. \tag{29}$$

The radial strain $\varepsilon_R$ has been calculated by using Eqs. (26)&(27), while the dependence of the fundamental frequency on the eardrum radius $a_{\text{tymp}}$ is accounted for by $\mu_{11}$ as defined in (5). For small strains, i.e., $\varepsilon_R \ll 1$, and small values of the applied tension $\mathscr{T}_{\text{app}} \ll T$, Eq. (28) reduces to a linear expression,

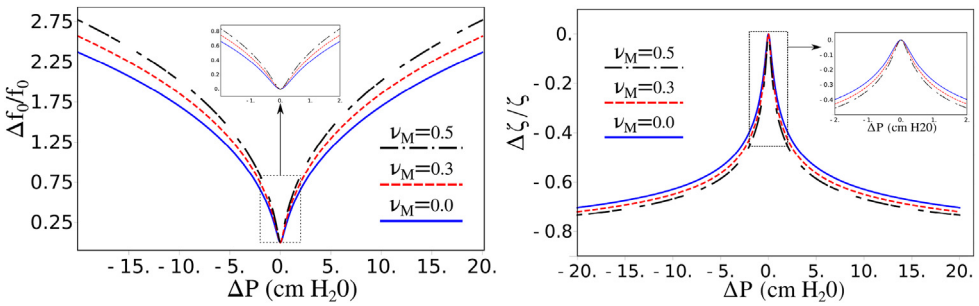


(a) $\Delta f_0/f_0$ vs. $\Delta P$ (b) $\Delta\zeta/\zeta$ vs. $\Delta P$

**Fig. 4.** (a) Relative change of the fundamental frequency $\Delta f_0/f_0$ with gular pressure $\Delta P$. The evenness of the curve around $\Delta P = 0$ is due to our assumption that the membrane is flat at its equilibrium position. Only for very large pressures ( $>5$ cm $H_2O$) does the dependence upon the Poisson ratio $\nu_M$ becomes apparent. The inset shows the dependence of $f_0$ upon smaller values of $\Delta P$ ( $<2$ cm $H_2O$). (b) Relative change of the damping ratio $\Delta\zeta/\zeta$ with gular pressure. According to Eq. (9), the damping ratio is given by $\zeta = \alpha/\omega_0$.

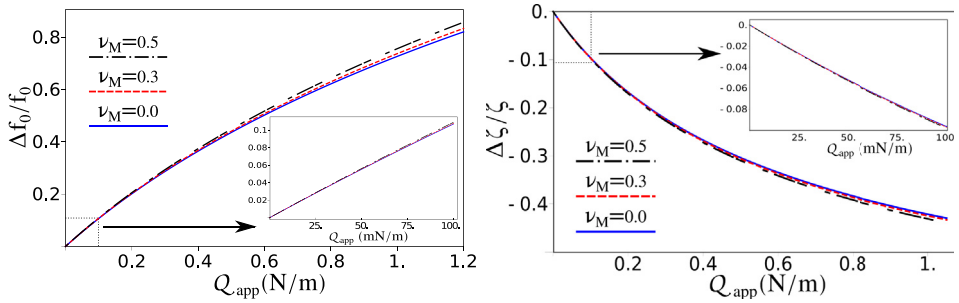


(a) $\Delta f_0/f_0$ vs. applied tension (b) $\Delta\zeta/\zeta$ vs. applied tension

**Fig. 5.** (a) Relative change of the fundamental frequency $\Delta f_0/f_0$ vs. applied tension $\mathcal{Q}_{app}$ in N/m for different values of the Poisson ratio $\nu_M$. A membrane of radius 3 mm, thickness 30 $\mu$m and an initial fundamental frequency $f_0 = 400$ Hz is subjected to a uniform radial tension $\mathcal{Q}_{app}$ via the tympanus muscle. The dependence upon the Poisson ratio $\nu_M$ is weak and only becomes apparent at higher values of $\mathcal{Q}_{app}$. For realistic values of the applied tension, i.e., when $\mathcal{Q}_{app}$ is small in comparison with the initial membrane tension $\sigma_0 \times d_M$, the relative shift $\Delta f_0/f_0$ is not sensitive to the value of $\nu_M$(Funnell and Laszlo, 1978) and has an approximately linear dependence upon $\mathcal{Q}_{app}$; see inset. (b) Relative change of the damping ratio $\Delta\zeta/\zeta$ with applied tension. As in the case of the gular pressure (see Fig. 4b), $\zeta$ decreases with the increase in $f_0$ brought about the applied tension $\mathcal{Q}_{app}$; cf. Eq. (9).

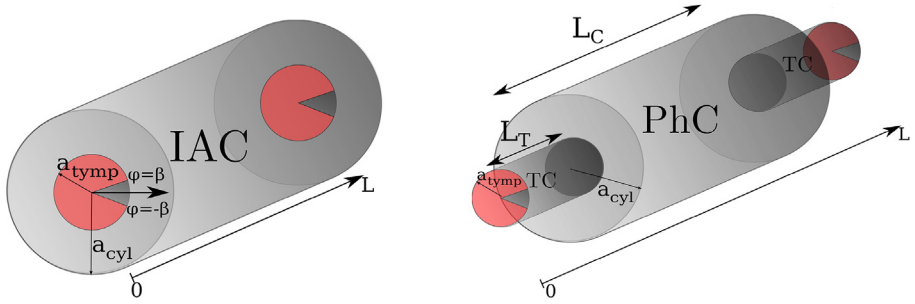


(a) Uniform diameter (b) Varying diameter

**Fig. 6.** (a) The ICE interaural cavity (IAC) modeled as an air-filled cylindrical cavity, whose radius $a_{cyl}$ is determined from the total volume of the interaural cavity, incorporating the tympanic and pharyngeal cavities. (b) The interaural cavity modeled as two cylindrical tympanic cavities (TC) coupled by means of a wider cylindrical pharyngeal cavity (PhC). The radius of the tympanic cavities is equal to that of the tympanic membranes, whereas the radius of the pharyngeal cavity is determined from its volume. Since for sound localization wavelengths $<16$ cm corresponding to frequencies $<2$ kHz are the relevant ones, this schematic description is justified.

$$\Delta f_0 = f_0\left(\frac{\mathcal{Q}_{app}}{2T} - \varepsilon_R\right). \tag{30}$$

*Note on the eardrum curvature.* As evidenced by Fig. 1, the *Varanid* eardrum is not flat but rather has a slight outward curvature resulting from the columella pushing on its interior surface through the extracolumella. Consequently, there is an apparent discrepancy between our flat-membrane description of the eardrum and its natural geometry. However, as the Appendix shows in detail, given the eardrum's flexible nature it acts like a drum and not like a spherical shell with spontaneous curvature, and its description as a flat membrane under tension is appropriate. Intuitively, we can immediately see this. The vibration mechanisms of bent and stretched membranes are illustrated by Fig. 13a and b.

The generic case of bending as the origin of biomembrane undulations is the cell membrane; for a review, one may consult van Hemmen and Leibold (2007). The thickness of the biomembrane (as phospholipid bilayer) is $h \approx 4$ nm, the cell size is $R \geq 10\mu$m, and undulation amplitudes are in a range of 30 nm, while the undulation wavelengths are appreciably smaller than $R$. Hence the membrane is strongly curved and bombarded by molecular Brownian motion with spatial fluctuations $\ll R$. Accordingly, membrane oscillations are generated by the mechanism depicted in Fig. 13a of the Appendix on a scale $\ll R$ so that its wavelengths are also smaller than $R$ and bending results; see, for instance, Marx et al. (2002, Fig. 1).

On the other hand, an eardrum of the "icy" animals analyzed here is macroscopic with $R \leq 3$ mm, their frequency range relevant for survival is $\leq 3$ kHz, with stimulus wavelengths $>10$ cm, so that the external stimulus pressure $p^{ext}$ is on average *uniform* over the eardrum. Natural vibration amplitudes are maximally 40 nm. As detailed in the Appendix, the eardrum is under tension. Its excitations are induced by a uniform stimulus pressure $p^{ext}$ and have amplitudes negligibly small as compared to $R$, which we can also consider as generous estimate of its radius of curvature (Fig. 1a).

Having an extremely small amplitude, the tympanic excitations are adequately described in the context of a linear theory by a superposition of the eigenfunctions of the tympanum, mathematically weighted by a scalar product of the tympanic eigenfunctions and $p^{ex}$ integrated over the manifold generated by the eardrum; there is even a systematic perturbation theory (Heider and van Hemmen, 2019) for the present situation, confirming what has just been formulated biophysically. Since the eigenstate corresponding to the eardrum's fundamental frequency is the only one that has no node lines and is practically uniform, it will deliver by far the biggest component in the tympanic motion. And it is completely immaterial whether we include the membrane curvature of order $1/R$ or treat the tympanic membrane as flat and under tension, as we have done; cf. the Appendix.

## 3. The pharyngeal cavity as a cylinder

In the first analytical description of ICE, the pharyngeal cavity was modeled as an air-filled cylindrical cavity coupling the two circular eardrums (Vossen et al., 2010). As the diameter of the

cylindrical cavity was equal to that of the eardrums and its length was equal to the interaural distance, the cavity volume was a fixed parameter of the model. In later treatments (Vedurmudi et al., 2016a, b), the volume of the cylindrical cavity was varied by changing the diameter of the cylinder while keeping its length constant; see Fig. 6a. Though Fig. 2 indicates that the shape of the pharyngeal cavity is different from a cylinder, the mathematical results we are going to obtain for the latter are also valid for the former. The generality of our arguments is due to an old principle of acoustics commonly referred to as the "$\lambda/16$ criterion" (Beranek, 1986), according to which spatial variations in the shape of the boundary smaller than $\lambda/16$ can be neglected, where $\lambda$ refers to the wavelength under consideration. In our case the relevant frequencies are below 1.5 kHz, implying that $\lambda/16$ exceeds 1.5 cm. In this range the cylindrical model is a faithful representation of biological reality.

In general, the internal pressure at the eardrum $p^{\text{in}}$ obeys the three-dimensional acoustic wave equation

$$\Delta_{(3)}p^{\text{in}} - \frac{1}{c^2}\frac{\partial^2 p^{\text{in}}}{\partial t^2} = 0 \tag{31}$$

where $c$ is the speed of sound in air. The particle velocity $\mathbf{v}$ derived from the linearized Euler equation is given by

$$\rho\partial\mathbf{v} \Big/ \partial t = -\nabla p^{\text{in}} \tag{32}$$

where $\rho$ is the quiescent density of air. The derivation of Eq. (32) from the Euler/Navier-Stokes equation is straightforward. The quadratic term $(\mathbf{v}.\nabla)\mathbf{v}$ in the Euler equation $\rho\partial\mathbf{v}/\partial t + (\mathbf{v}.\nabla)\mathbf{v} = -\nabla p^{\text{in}} + \mathbf{F}$ can be neglected because of small amplitudes in natural surroundings. In the present case the force field $\mathbf{F}$ is also vanishing. On the tympanic surface, we have no-slip boundary conditions so that the air-velocity on the surface equals the eardrum velocity (2). Because of the extremely small ($\sim$ nm) amplitudes of the eardrum vibration, only the component of $\mathbf{v}$ normal to the eardrum surface, i.e., $\partial u/\partial t = \mathbf{n}.\mathbf{v}$ is non-zero. Here $\mathbf{n}$ is the normal vector and $u$ is the eardrum vibration amplitude appearing in Eq. (2). In summary, the membrane dynamics is described by the damped wave equation (2) with $p^{\text{ex/in}}$ as the driving source terms. On the other hand, the wave equation describing $p^{\text{in}}$ (31) contains the fluctuating eardrums as its boundary terms that generate the pressure dynamics. In this way, the tympanic membranes influence the dynamics of $p^{\text{in}}$. In fact, the vibration of the tympanic surface also results in a variation of the pharyngeal cavity's volume. The details of the full mathematical problem of the coupled vibrations of the eardrums and pharyngeal cavity can be found in Heider and van Hemmen (2019).

For a cylindrical cavity as depicted in Fig. 6a, the air velocity and pressure vary along the coordinates $\{r, \phi, x\}$, where $x$ denotes the coordinate along the cylinder axis and $\{r, \phi\}$ are the polar (radial and azimuthal) coordinates orthogonal to it. At low frequencies, the variation in the radial and azimuthal directions can be neglected so that, at a given frequency $f = \omega/2\pi$, the pressure $p$ and velocity $v$ can be described by plane waves,

$$p^{\text{in}}(x;t) = \left(Ae^{ikx} + Be^{-ikx}\right)e^{i\omega t}\,, \tag{33}$$

$$v(x;t) = \frac{-1}{\rho c}\left(Ae^{ikx} - Be^{-ikx}\right)e^{i\omega t}\,. \tag{34}$$

Here $k = \omega/c$ is the wave number corresponding to the frequency $f$. The previous results are in fact derived using the piston approximation (Vedurmudi et al., 2016a, b), where the motion of the eardrum surface is approximated by a piston moving with the average velocity of the eardrum surface including the non-moving surface of the cylinder; cf. Fig. 6a. As a result, $p^{\text{in}}$ is proportional to the average displacement $u^{\text{ave}}$ (Vedurmudi et al., 2016a, b) and can be expressed in terms of coefficients $\Gamma_\pm$

$$2p^{\text{in}}_{0/L} = \Gamma_+(u^{\text{ave}}_L \mp u^{\text{ave}}_0) + \Gamma_-(u^{\text{ave}}_L - u^{\text{ave}}_0) \tag{35}$$

where the indices $0/L$ denote the positions of the two eardrums. For a cylindrical interaural cavity of length $L$ and volume $V_{\text{cav}}(= \pi a^2_{\text{cyl}}L)$, the internal pressure coefficients are given by (Vedurmudi et al., 2016b)

$$\Gamma_+ = -\frac{\rho c^2}{V_{\text{cav}}}kL\cot kL \Big/ 2\,,\ \Gamma_- = \frac{\rho c^2}{V_{\text{cav}}}kL\tan kL \Big/ 2\,. \tag{36}$$

The eardrum vibrations in response to an external and internal sound pressure can be written in terms of the frequency response $\Lambda$ (7),

$$u^{\text{ave}}_{0/L} = \Lambda\left(p^{\text{ex}}_{0/L} - p^{\text{in}}_{0/L}\right). \tag{37}$$

The above equations can now be used to express the eardrum displacements as a function of the external pressure,

$$2\,u^{\text{ave}}_{0/L} = \frac{(p^{\text{ex}}_L + p^{\text{ex}}_0)}{1/\Lambda + \Gamma_+} \mp \frac{(p^{\text{ex}}_L - p^{\text{ex}}_0)}{1/\Lambda + \Gamma_-}. \tag{38}$$

*Varying the cavity volume.* According to Eq. (36), a change in the cavity volume $V_{\text{cav}}$ is reflected in the coefficients $\Gamma_\pm$. A homogeneous increase in the interaural cavity volume is, however, not fully consistent with the true anatomy of the animal as the expansion of the gular only increases the volume pharyngeal cavity *locally*. In order to account for this fact, we instead model the interaural cavity as two narrow cylindrical tympanic cavities (TC) coupled by means of a wider pharyngeal cavity (PhC); cf. Fig. 6b. Thus, a variation of the cavity volume only changes the diameter of the pharyngeal cavity. Expressions for the internal pressure were calculated for a cavity with varying diameter, albeit one with conical tympanic cavities coupled by a narrow cylindrical internal canal in the African clawed frog *Xenopus laevis* (Vedurmudi et al., 2018). For the relatively simpler case of cylindrical canals, the corresponding $\Gamma_\pm$ coefficients can be found by solving the acoustic wave equation (31) independently in the tympanic and pharyngeal cavities resulting in separate plane waves similar to Eq. (33) in each section. We then require the continuity of pressure and the conservation of volume flow (velocity $\times$ cross section) at the junctions between the tympanic and pharyngeal cavities. For a geometry with cylindrical tympanic cavities of cross section $S_{\text{T}}$ and length $L_{\text{T}}$, connected via a cylindrical pharyngeal cavity of cross section $S_{\text{C}}$ and length $L_{\text{C}}$ (cf. Fig. 6b), the corresponding coefficients are given by

$$\tilde{\Gamma}_+ = \frac{\rho c^2 k}{S_{\text{T}}}\frac{(S_{\text{C}}\tan(kL_{\text{T}})\tan(kL_{\text{C}}/2) - S_{\text{T}})}{(S_{\text{C}}\tan(kL_{\text{C}}/2) + S_{\text{T}}\tan(kL_{\text{T}}))} \tag{39}$$

and

$$\tilde{\Gamma}_- = \frac{\rho c^2 k}{S_{\text{T}}}\frac{(S_{\text{C}}\tan(kL_{\text{T}}) + S_{\text{T}}\tan(kL_{\text{C}}/2))}{(S_{\text{C}} - S_{\text{T}}\tan(kL_{\text{T}}))\tan(kL_{\text{C}}/2)}\,, \tag{40}$$

such that the interaural separation is given by $L = 2L_{\text{T}} + L_{\text{C}}$. It is a simple algebraic exercise to verify that $\tilde{\Gamma}_\pm$ reduces to $\Gamma_\pm$ when $S_{\text{C}} = S_{\text{T}}$.

While the influence of the cavity volume $V_{\text{cav}}$ on the internal pressure is manifest in the expressions for $\Gamma_\pm$ as given by (36), the direct dependence of $\Gamma_\pm$ is on the cross section $\pi a^2_{\text{cyl}}$ of the cylinder.

This is due to the fact that in our model the interaural distance $L$ is constant and the volume of the interaural cavity is given by

$$V_{\text{cav}} = \pi a_{\text{cyl}}^2 L \,. \tag{41}$$

In contrast, for the localized dilation of the interaural cavity we require that only the cross-section of the pharyngeal cavity $S_{\text{C}}$ is variable; see Fig. 6b. Keeping the lengths of the individual cavities $L_{\text{T/C}}$ and the cross section of the tympanic cavity $S_{\text{T}}$ constant, the variation of the pharyngeal cross section with respect to the total cavity volume is given by

$$S_{\text{C}} = (V_{\text{cav}} - 2S_{\text{T}}L_{\text{T}}) \,/\, L_{\text{C}} \,. \tag{42}$$

Thus, varying the volume of the interaural cavity via a localized dilation of the pharyngeal cavity corresponds to the variation of the cross section $S_{\text{C}}$, while keeping the interaural distance $L$ and tympanic cavity cross section $S_{\text{T}}$ constant. In this way the influence of $V_{\text{cav}}$ on $\tilde{\Gamma}_{\pm}$ via a variation in the pharyngeal-cavity cross section $S_{\text{T}}$ is evident from Eqs. (39) and (40).

### 3.1. Sound input

In animals with ICE, the typical head size is at most 10 cm and, hence, small relative to the sound wavelengths that convey relevant information. Consequently, there is negligible diffraction and acoustic shadowing around the head and, as shown by (38), the external sound inputs to the ears only differ in interaural time delay (or phase) and not in amplitude (Michelsen and Larsen, 2008). The general expressions for the sound inputs that serve as the external driving pressure for the eardrums (2) read Vedurmudi et al. (2016a).

$$p_{0/L}^{\text{ex}} = p\exp(i\omega t)\exp(\mp ik\Delta \,/\, 2) \,, \tag{43}$$

where $k = \omega/c$ is the wavenumber an angular frequency $\omega = 2\pi f$ and $c \approx 330$ m/s is the speed of sound in air. For an interaural separation $L$, $\Delta = L\sin\theta$ is the additional distance traveled by a sound wave to reach the opposite ear; see Fig. 7.

In general, the external sound pressure $p^{\text{ex}}$ is also influenced by the vibration of the eardrum. However, this effect is considerably more pronounced in the case of underwater hearing due to the eardrum's acoustic radiation inducing a pressure on its surface (see Vedurmudi et al. (2018) for the case of *Xenopus*). Moreover, as the *Varanus* eardrum is located superificially, the acoustic effects of its shallow ear canal can be neglected for its hearing range. As a result, $p^{\text{ex}}$ in our case is determined almost entirely by the external sound source. On the other hand, as the interaural cavity is shielded from the external sound, the internal pressure $p^{\text{in}}$ is a function of the eardrum vibrations alone (36) and only depends on the external sound pressure indirectly.

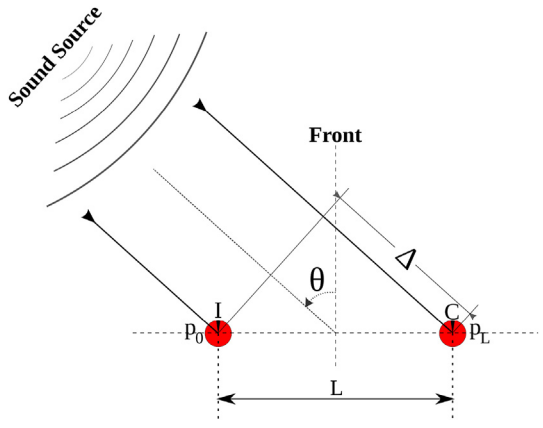


**Fig. 7.** Acoustic head model with interaural distance $L$( $\ll$ distance to sound source) for *Varanus* with $L \approx 3$ cm. The extra distance traveled by the sound wave from a direction $\theta$ to reach the **C**ontralateral ear is given by $\Delta = L\sin\theta$. Given an external tone with frequency $f$, wavelength $\lambda$, and hence $k = 2\pi/\lambda$, this gives rise to a phase difference $\Phi = kL\sin\theta$ from the input at the **I**psilateral ear. Here $\theta = 0$ corresponds to a source in front of the animal while $\theta = \pm 180^\circ$ corresponds to the one right behind it.

## 4. Sound localization cues

For the external input to the ears, the directional information is available in the form of an interaural level (or amplitude) difference (**I**LD) and an interaural time difference (**I**TD) corresponding, for a pure tone, to the phase difference between the inputs. Because of the interaural coupling, however, the amplitude and time difference between the vibrations of the eardrums are modified to *internal* time (**i**TD) and level (**i**LD) differences that are experienced and evaluated by the auditory system and in general are different from the external ITD and ILD.

The biological physics of hair-cell response is governed by the Weber-Fechner logarithm of the amplitude. Accordingly, the iLD and ILD are quantified by

$$\text{iLD} = 20\log_{10}\left|\frac{u_L^{\text{ave}}}{u_0^{\text{ave}}}\right|, \qquad \text{ILD} = 20\log_{10}\left|\frac{p_L^{\text{ex}}}{p_0^{\text{ex}}}\right|. \tag{44}$$

In our model, as $p_0^{\text{ex}}$ and $p_L^{\text{ex}}$ have practically the same amplitude, the ILD vanishes; cf. Eq. (43)&(44).

In animals with ICE, it is also possible to significantly increase the phase difference or, equivalently, the time difference between the eardrum vibrations Vossen et al. (2010); Vedurmudi et al. (2016a). The iTD, the internal time difference between the two eardrums as measured by the columellae, is defined as the phase difference between the inputs to the ears divided by the angular frequency $\omega = 2\pi f$ with, as usual, $f$ as frequency. Unlike the ITD, which is independent of frequency, the internal time difference is, in general, frequency dependent. The iTD and ITD can be written in terms of the eardrum vibrations and input pressures, respectively,

$$\text{iTD} = \text{Arg}\left(\frac{u_L^{\text{ave}}}{u_0^{\text{ave}}}\right) \Big/ \omega, \qquad \text{ITD} = \text{Arg}\left(\frac{p_L^{\text{ex}}}{p_0^{\text{ex}}}\right) \Big/ \omega \,. \tag{45}$$

The iTD and iLD will subsequently serve as a metric for quantifying the directional response of our model. Given the sound speed $c$, the interaural time difference can also be directly expressed as ITD $= L \sin\theta/c$.

### 4.1. Influence of system parameters on iTD & iLD

The fundamental frequency $f_0$ and the damping coefficient $\alpha$ play a fundamental role in determining the frequency behavior of the sound localization cues in animals with ICE. The transition from the low-frequency regime corresponding to the use of iTDs to the high-frequency regime corresponding to strong iLDs is determined by $f_0$ (Vedurmudi et al., 2016a, b). Below $f_0$ there is a plateau of the fraction iTD/ITD = TDF, the time dilation factor, which often rises to 3–4. Just above $f_0$ there is at angles $\pm 90^\circ$ often an outspoken maximum of the iLD, which may be 10–20 dB, even though the interaural level difference ILD is practically always vanishing.

Moreover, for a given $f_0$ the value of the damping coefficient controls both the shape of the time dilation factor or TDF (iTD/ITD) plateau and the peak value of the iLD; see Fig. 8. For large values of $\alpha$, the iTD decreases with frequency, whereas for smaller values of $\alpha$, the iTD at first increases with frequency and then sharply drops

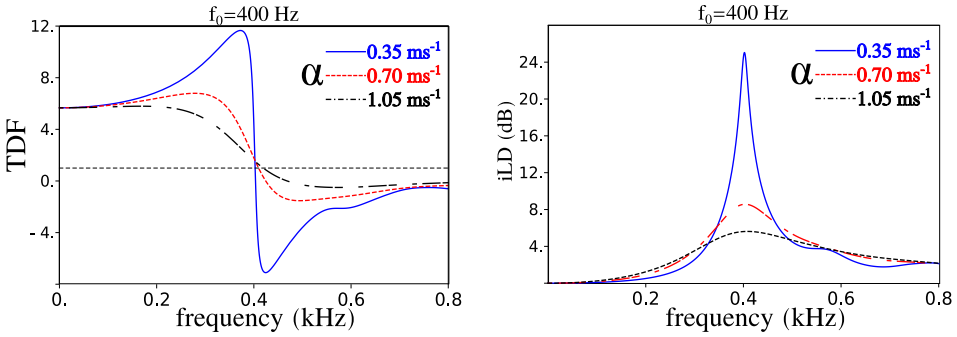


(a) TDF vs. frequency for different $\alpha$ (b) iLD vs. frequency for different $\alpha$

**Fig. 8.** Variation of the (a) time dilation factor (TDF = iTD/ITD) and (b) internal level difference (iLD) with the membrane damping factor $\alpha$ for a *Varanus*-like eardrum with the fundamental frequency fixed at $f_0 = 400$ Hz. We see that a significant damping is necessary to ensure a low-frequency plateau in the TDF, which is conducive to iTD sound localization. Nevertheless, the plateau width is restricted, viz., at best up to 200 Hz for $\alpha = 1.05\ (\text{ms})^{-1}$. Furthermore, the damping does not influence the absolute value of the TDP plateau at low frequencies. The trade-off, as can be seen in the frequency dependence of the iLD, is that an increase in $\alpha$ significantly reduces the iLD peak.

around $f = f_0$.

Fig. 9 shows the frequency dependence of the TDF (= iTD/ITD) and iLD for different values of $f_0$. We see that an increase in $f_0$ results in a decrease in the "height" of the TDF plateau with a simultaneous increase in the width of its frequency range. On the other hand, increasing $f_0$ results in a shift the iLD peak frequency, with a small decrease (compared to the TDF) in the maximum value of the iLD. This indicates that the sensitivity to iLD cues can be tuned by varying the tension of the eardrum, albeit with a reduction in the corresponding TDF as a trade-off.

The dependence of TDF and iLD upon the membrane tension $T$ is further illustrated in Fig. 10 for different sound-source directions. For all directions, there is a decrease in the TDF with an increase in membrane tension, whereas the iLD remains practically constant. The implication of this behavior is that, while the tympanus muscle can be used to effectively tune the iLD peak frequency and thus the corresponding optimal frequencies for sound localization, a resulting trade-off in the form of a reduced iTD is necessary. In other words, varying the tension of the eardrum changes the efficiency of any iTD-based sound localization afforded by the width of a constant TDF = iTD/ITD plateau.

### 4.2. Influence of cavity volume on iTD & iLD

From Eqs. 36–40 it is clear that the cross section of the cylindrical cavity, and thus the cavity volume $V_{\text{cav}}$ plays a fundamental role in determining the nature of the interaural coupling between the eardrums. As *Varanus* is capable of *locally* varying the volume of the interaural cavity, it is worthwhile to ascertain whether a localized increase of the cavity volume is advantageous, as opposed to a uniform increase in the same. The geometry of the interaural cavity for the two scenarios was illustrated in Fig. 6.

Fig. 11a shows the variation of the TDF (low-frequency limit) for a sound source direction $\theta = 90^\circ$ with cavity volume for the cases of uniform and localized dilation of the cylindrical cavities in terms of a "minimal" reference volume which we define as

$$V_{\text{min}} = \pi a_{\text{tymp}}^2 L\,.$$

The "minimal" volume for a cylindrical cavity arises from the fact that the radius of the cavity is bound to be greater than that of the eardrum. An increase in $V_{\text{cav}}$ is accompanied by a steady decrease in the maximum value of the TDF. The behavior of the TDF is determined largely by the volume of the cavity, as opposed to its shape. This is reflected in the identical curves for uniform and localized dilation and is due to the fact that, at low frequencies and hence long wavelengths, the exact geometry of the cavity is irrelevant.

An increase in the TDF at lower cavity volumes, however, is also accompanied by a loss of the TDF plateau (Vedurmudi et al., 2016b); see Fig. 11b. A TDF plateau is essential for sound localization using iTDs, as it signifies that the time difference between the eardrum

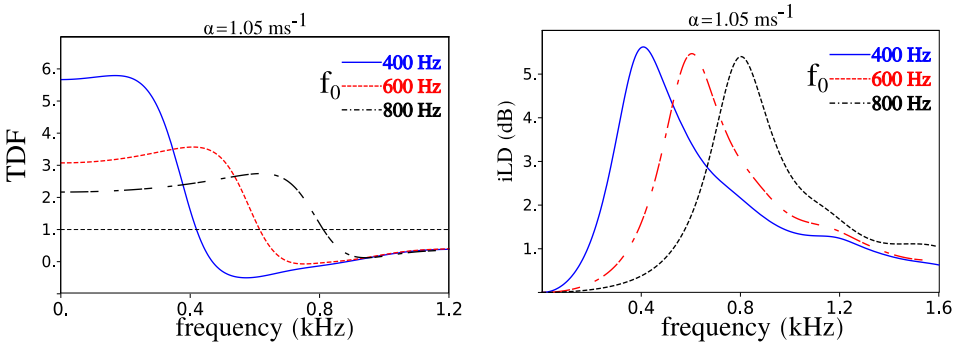


(a) TDF vs. $f$ for different $f_0$ (b) iLD vs. $f$ for different $f_0$

**Fig. 9.** Variation of the (a) time dilation factor (TDF = iTD/ITD) and (b) internal level difference (iLD) with the membrane frequency $f_0$ for a *Varanus*-like eardrum with the damping fixed at $\alpha = 1.05\ (\text{ms})^{-1}$ Hz. Increasing the fundamental frequency extends the TDF plateau, while at the same time reducing its height. On the other hand, the value of the peak of the iLD decreases only slightly with an increase in the fundamental frequency, whereas its peak shifts significantly with $f_0$. This indicates the possibility of tuning the sensitivity to sound localization cues by changing the tension of the eardrum; for instance, by contraction of the tympanus muscle.

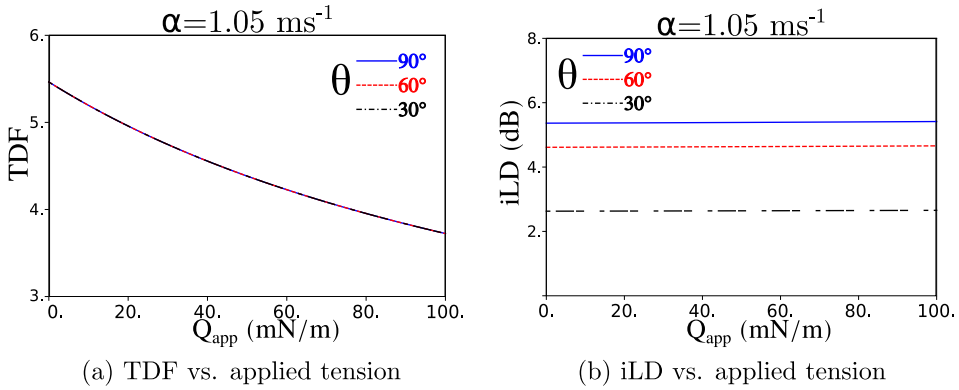


(a) TDF vs. applied tension (b) iLD vs. applied tension

**Fig. 10.** Variation of the (a) TDF (iTD/ITD) at $f = 100$ Hz and (b) internal level difference at $f = f_0$ with the membrane tension for a *Varanus*-like eardrum with the damping fixed at $\alpha = 1.05\text{ms}^{-1}$. In the above plots, the results of Figs. 8 and 9 are clearly visible. Given the variation $\Delta f_0$ of the fundamental frequency $f_0$ with the applied tension $\mathscr{T}_{\text{app}}$ as given by Eq. (28), we see that, while the TDF decreases steadily with increasing tension, the iLD remains practically constant. For the TDF, the curves corresponding to different angles coincide as the TDF does not depend on the source direction for low frequencies (Vedurmudi et al., 2016a).

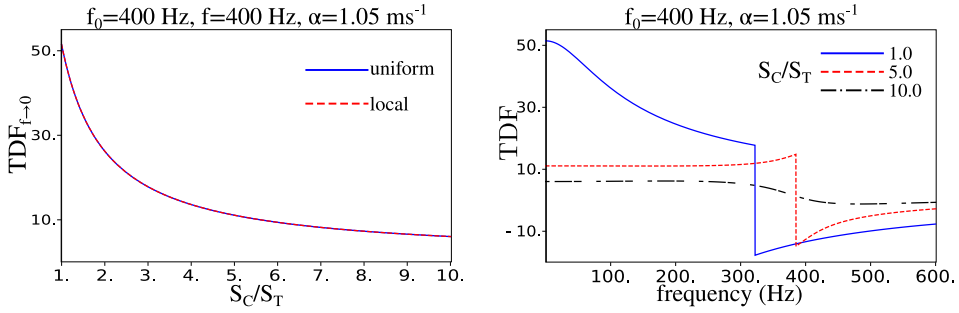


(a) $\text{TDF}_{f\to 0}$ vs. cavity volume (b) TDF plateau vs. cavity volume

**Fig. 11.** (a) Zero-frequency limit of the TDF = iTD/ITD for a uniform and localized dilation of the cylindrical cavity; cf. Fig. 6. (b) Frequency dependence of the TDF for different cavity volumes. At low volumes, the high TDF at low frequencies is accompanied by a loss of the plateau.

vibration only depends on the direction of the sound source and not its frequency characteristics, thus mirroring the behavior of the interaural time difference (45).

The variation of the maximum iLD for a given cavity volume is shown in Fig. 12a for a sound-source direction $\theta = 90^\circ$. The apparent singularity at around $V_{\text{cav}} \approx 6V_{\text{min}}$ corresponds to the "critical" volume of the system (Vedurmudi et al., 2016b), where the internal and external pressures at the contralateral eardrums become equal, resulting in a zero-vibration amplitude. Consequently, the iLD, which is calculated as the logarithm (44) of the ratio of vibration amplitudes, diverges. As in the case of the TDF (see Fig. 11), both a uniform and localized dilation of the cylinder do not differ significantly in terms of their influence on the iLD.

The frequency corresponding to the maximum iLD for a given cavity volume is shown in Fig. 12b for both a uniform and a localized dilation of the interaural cavity. In both cases, there is a clear inflection point where the behavior of the iLD transitions from a sub-optimal low-volume regime to a more ICE-like high volume

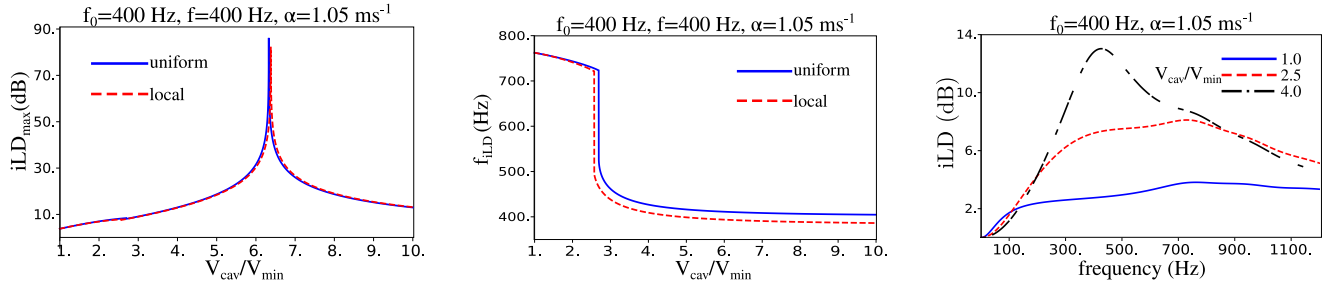


(a) Max iLD vs. cavity volume (b) Frequency of max iLD vs. $V_{\text{cav}}$ (c) iLD vs. cavity volume

**Fig. 12.** (a) Variation of the maximum iLD for sound source direction $\theta = 90^\circ$ in dependence upon the cavity volume for a uniform and localized dilation of the interaural cavity. There is no significant difference between the two cases, although a localized dilation results in a slightly lower maximum iLD. The singularity around $V_{\text{cav}} \approx 6V_{\text{min}}$ corresponds to the critical volume of the cavity, where the contralateral eardrum stops vibrating. (b) Frequency of maximum iLD with cavity volume. The distinct change in $f_{\text{iLD}}$ corresponds to a transition from a sub-optimal region to a region with more ICE-like behavior. (c) The transition can be more clearly seen via the frequency dependence of the iLD for different values of $V_{\text{cav}}$. A peak in the iLD at around $f = f_0 = 400$ Hz emerges for a cavity volume between $2.5V_{\text{min}}$ and 4min.

regime. This can be seen more clearly in Fig. 12c, where the emergence of a peak at around $f_0 = 400$ Hz is clearly seen between cavity volumes $2.5V_{\min}$ and $4V_{\min}$. At lower volumes the influence of the fundamental mode $f_0$ as given by (5) is suppressed, resulting in a peak close to 800 Hz, corresponding to the second frequency mode $f_1$,

$$f_1 = \frac{c_M \mu_{12}}{2\pi} = \frac{\mu_{12}}{2\pi}\sqrt{T/\rho_M d_M}\,. \tag{46}$$

## 5. Discussion

The Asian water monitor *Varanus salvator* has the ability to vary its eardrum tension both by means of the tympanus muscle on its eardrum periphery and by ventilating its gular. A mechanical model for the asymmetrically loaded reptilian eardrum has been used to describe the middle ear system of *Varanus*. In the case of gular expansion, a pressure difference between the internal and external surfaces of the eardrum results in an outward or inward distention changes the eardrum tension and, as a result, its fundamental frequency $f_0$. Thus, the increase in tension due to an increase of the eardrum surface area compensates for the pressure difference due to gular ventilation; cf. Eq. (12).

In contrast, the tympanus muscle can be used to induce a radial stretching of the eardrum resulting in an increased tension and, as a consequence, an increased $f_0$; see also Eq. (28). In both cases, the change in $f_0$ has been found to be independent of the Poisson ratio $\nu_M$ of the eardrum for values of gular pressure difference and applied tension corresponding to realistic values for the animal; see Figs. 4a and 5a. Moreover, for small values, the change $\Delta f_0$ in the fundamental frequency was found to vary linearly with the tension $\mathscr{E}_{\text{app}}$ as given by (30), suggesting a greater degree of control on $f_0$ with the tympanus muscle in comparison with the gular pressure.

Because *Varanus* is equipped with internally coupled ears (ICE), the hearing cues available (internal time and level difference or iTD & iLD) are enhanced in comparison to the cues available solely from the external inputs (interaural time and level difference or ITD & ILD). As the frequency dependence of hearing cues is intimately connected with the eardrum's material properties, the ability of *Varanus* to actively vary its eardrum tension has fundamental implications for not just its hearing, but also for its sound localization ability.

Since the iLD as given by Eq. (44) shows a peak when the sound input frequency is quite close to the eardrum's fundamental frequency $f_0$, *Varanus* can vary the position of the iLD peak by varying its eardrum tension; see Fig. 9b. Moreover, the height of the iLD peak is insensitive to $f_0$ or, equivalently, to the eardrum's tension $T$ (Fig. 10b). Varying the tension is achieved by the *tympanus* muscle (Fig. 1b).

On the other hand, the internal time difference or iTD as given by (45) shows a greater degree of sensitivity to the eardrum tension than the iLD. As $f_0$ increases, the height of the TDF = iTD/ITD plateau decreases, as does the "flatness" of the plateau in Figs. 9a and 10a. This implies that the ability to tune the iLD peak results in a trade-off where the ability of the animal to localize a sound source using iTDs is increasingly impaired. Experimentally, the values of the iTD (and, hence, the TDF) as well as the iLD are accessible straightforwardly via laser-vibrometry measurements of the eardrum (Christensen-Dalsgaard and Manley, 2005, 2008). Any variation in the TDF plateau or the position of the iLD maximum would indicate the animal's ability to actively modulate its sound-localization ability.

A localized gular expansion (see Fig. 6b) as opposed to a global increase in the cavity volume (Fig. 6a) has nearly no bearing on the frequency dependence of the iTDs and iLDs (Figs. 11b and 12a). However, the absolute value of the interaural cavity $V_{\text{cav}}$ has significant effects on both iTD and iLD. A small cavity volume increases the maximum iTD at low frequencies but results in a deterioration of the plateau (Fig. 11b). In the iLD case, the peak around $f_0$ disappears below a certain "critical" volume $V_{\text{crit}}$ (Fig. 12b and c). Both results are in agreement with previous observations for geckos (Vedurmudi et al., 2016b), where the optimal interaural cavity volume, at which a flat TDF plateau is accompanied by high iLDs, is just above $V_{\text{crit}}$ (Vedurmudi et al., 2016b).

## Acknowledgements

JLvH acknowledges travel funding from the German Ministry of Education and Research (BMBF) through Bernstein Center for Computational Neuroscience – Munich (Bernstein II).

## Appendix. Curvature vs. tension and oscillations

Glancing at Fig. 1a one is inclined to think of the eardrum of a water monitor as what is referred to in technical applications as a spherical cap or shell. Sound hits the eardrum and sets it into motion. How, then, do we mathematically describe these tympanic, transverse, oscillations induced by sound? That is the question we are going to analyze from two different points of view. First, we focus on small oscillations in a spherical cap or shell with spontaneous curvature, a technical problem that has been analyzed and solved in full detail by Eric Reissner (Reissner, 1955, 1996; Johnson and Reissner, 1958) in the 1950s and by many authors after him; see in particular Timoshenko's classic (Timoshenko and Woinowsky-Krieger, 1959). We will contrast this setup to a drum, an elastic membrane under tension. Despite Fig. 1a looking different, we will see that the eardrum is really a drum. Here too, appearances are deceiving. Whatever the driving mechanism, there is, however, a unifying element: For oscillations to arise, a medium needs restoring forces back to equilibrium while doing so back and forth – during oscillation. We are going to analyze two of them, bending a plate and stretching a string.

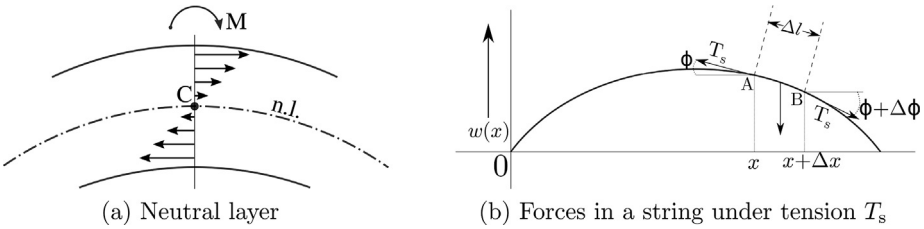


(a) Neutral layer (b) Forces in a string under tension $T_s$

**Fig. 13.** (a) Intersection of a plate bent downwards. A key notion of bending a relatively thin plate is the neutral layer (n.l.), above which the filaments are stretched whereas below they are squeezed. If the plate is bent upwards, the filaments below are stretched whereas above are squeezed. Both stretching and squeezing of material generates opposite forces that drive the material back to equilibrium; that is in this case, downwards. (b) Forces on a small piece of a string under tension of strength $T_s$ between $x$ and $x + \Delta x$. In both cases the restoring forces induce oscillations.

Let us start with a membrane that we imagine as a relatively thin spherical cap of thickness $h$; see Figs. 1a and 3a. We assume the rim to be fixed (i.e., Dirichlet boundary conditions) and positioned at the level $z = 0$ of the $\{x, y\}$ plane, where it is fixed but can rotate freely so that no torque exists (i.e., 2nd derivative in normal direction $= 0$). The present boundary conditions correspond to the way in which *Varanus*'s eardrum is attached the bones that surround it. Young's modulus $E$ is so large that the membrane is hard to stretch but relatively easy to bend. Cell membranes are of this type and have been modeled in a generality (van Hemmen and Leibold, 2007) that we do not need here. Since all these eardrum surfaces are curved, the Laplace operator is often (van Hemmen and Leibold, 2007) a Laplace-Beltrami operator but the latter won't appear here either. Instead a sufficiently accurate description is provided by Eq. (47) below.

The physics underlying oscillations in a plate of the above type and of finite thickness is subtler than one might naively believe. On bending the plate there turns out to be a so-called *neutral layer*. If the plate is bent downwards, filaments above the neutral layer are stretched and those below are squeezed, whereas in the neutral layer they are neither; see Fig. 1b. The material being elastic, it will try to – so to speak – expand below and contract above the neutral layer; this is the oscillation mechanism. While the plate is oscillating, expansion and contraction alternate.

The equations of motion are in general derived from a variational principle. The Lagrangian consists of kinetic and potential energy. The former is a simple one and generated by normal motion only. If the normal coordinate is $\psi$, then the kinetic energy is of the dimensionality mass times velocity squared and, thus, $\int_{\mathscr{M}} \mathrm{d}S \rho (\partial_t \psi)^2$ where $\mathscr{M}$ is the two-dimensional tympanic manifold with surface measure $\mathrm{d}S$ while $\rho$ is a mass density, i.e., mass per unit area. The potential energy either can be written down as an ansatz (Helfrich, 1973) in terms of a second-order (quadratic) polynomial in the principal curvatures $\kappa_1$ and $\kappa_2$ or is to be derived mechanistically, as has been done by, e.g., van Hemmen and Leibold (2007, Fig. 4 & Eqs. 16–19).

The equations of motion then result from the variational principle as described above and applied to the Lagrangian one has obtained. Let the Cartesian variables $\{x, y\}$ serve as the parametrization of the shell $\mathscr{M}$ and let $z(x, y)$ describe the neutral layer of the spherical shell, the two-dimensional manifold $\mathscr{M}$. Furthermore, let $E$ be Young's modulus and $D = Eh^3/12(1-\nu^2)$ the bending stiffness (or bending rigidity $k_c$ (van Hemmen and Leibold, 2007, Eq. (18))) with $\nu \equiv \sigma$ as Poisson's ratio. As before, let $h$ be the shell's thickness. Finally, we use the shorthand $\partial_x = \partial/\partial x$, etc. In the present case we then find (Reissner, 1955, Eqs. (I) & (II)) two simultaneous equations for $F$ and $w$, where $w$ is the vertical (practically normal) displacement,

$$\Delta^2 F = Eh\left[2\left(\partial_x\partial_y z\right)\,\partial_x\partial_y w - \partial_x^2 z\,\partial_y^2 w - \partial_y^2 z\,\partial_x^2 w\right], \tag{47}$$

$$\begin{aligned} D\Delta^2 w + (\rho h)\,\partial_t^2 w = -\Big[&2\left(\partial_x\partial_y z\right)\,\partial_x\partial_y F \\ &\Big[ - \partial_x^2 z\,\partial_y^2 F - \partial_y^2 z\,\partial_x^2 F\Big]. \end{aligned} \tag{48}$$

The dynamics is in $w$ and is governed by $\Delta^2$ in (48) while its source term $F$ in (47) is an auxiliary variable, Airy's stress function (as it was called in Reissner's days), that is determined mainly by the curvature of the manifold $\mathscr{M}$ supplemented by $w$. It has to be borne in mind that $z(x, y)$ describes the neutral layer of the cap, viz., $\mathscr{M}$.

The above two equations (47) and (48) dating back to Reissner (Reissner, 1955, 1996; Johnson and Reissner, 1958) describe transverse vibrations in rotationally symmetric, "spherical," shells with spontaneous curvature and without internal stress. In the present context, there are three physical parameters to be taken care of: the typical amplitude $A$ of the excitations involved, the membrane thickness $h$, and the extent $R$ of the object that confines the oscillations, in our case the eardrum.

*Dimensional analysis.* For a cell membrane, which can be described to perfection by the theory of elastic plates (van Hemmen and Leibold, 2007, §1 and Fig. 1), we have the cell size $R$ and $h << A \leq R$. It is important to realize that the elementary excitations are described in terms of the first few eigenstates of an in general slightly more general operator (van Hemmen and Leibold, 2007, Eq. (153)) than $\Delta^2$ on the manifold $\mathscr{M}$ and with radii of curvature appreciably smaller than $R$. In fact, $A/h << 1$ with $A$ of the order of 40 nm while $h \approx 4$ nm; see, for instance, Marx et al. (2002, Fig. 1). Hence, the energy is induced by curvature or, in plain English, by bending.

On the other hand, for a tympanic membrane we have $A \leq 50$ nm (the upper bound corresponding to disco sound), accordingly $A << h << R$, and thus $A/h >> 1$. That is, the latter situation faces a totally different kind of (biological) physics that is driven by tension and not by curvature. If one excises the extracolumella, a fluffy flat structure without spontaneous curvature remains. The eardrum is put under tension through the columella that connects the extracolumella to the cochlea's oval window and puts the eardrum under tension so that, once the eardrum moves, all vibrations are transmitted to the cochlea. In other words, the eardrum is always a drum, despite its dome-shaped structure as it occurs here.

Since tympanic amplitudes are in the nanometer range whereas the eardrum itself has a typical size $R$ in the cm range, the curvature practically does not change and the mechanism driving the system back to equilibrium is the membrane tension $T$. To see where the two-dimensional Laplacian, i.e., the second derivative, comes from, we turn to a quick derivation for a one-dimensional membrane, which is the usual string; see Fig. 13b. We then grant us the second dimension by analogy.

*Dynamics: strings and drums.* The string's deviation from equilibrium ($= 0$) in vertical direction is denoted by $w(x)$. At $x$ the *string* tension $T_\mathrm{s}$ pulls upwards to the left and makes a small angle $\varphi$ with the $x$-axis (for the sake of clarity not small in the plot) whereas at $x + \Delta x$ it pulls downwards with angle $\varphi + \Delta\varphi$. As $\varphi$ is small, $\sin\varphi = \varphi = \tan\varphi$ and we effectively get a force $-\varphi T_\mathrm{s}$ pulling downwards in vertical direction. For negative $w(x)$ we would get $\varphi T_\mathrm{s}$ pulling upwards. Hence in both cases we obtain a force trying to restore equilibrium. Without damping, there is a steady overshooting and oscillation prevails.

Because there is only one dimension and thus one free coordinate $x$, we look for the forces operating on a piece of string between $x$ and $x + \Delta x$. Its mass is $\rho\Delta x$ (as $\varphi$ is small) and, since we are at $x$, we indicate its time-dependent vertical coordinate by $w(x, t)$. According to Newton's law, $(\rho\Delta x)\,\partial_t^2 w$ equals the force on the mass $\rho\Delta x$, which we now compute.

In equilibrium the string is straight and uniform but in a small-amplitude transverse wave and under the tension $T_\mathrm{s}$, which is present everywhere in the string and, since the string is uniform, $T_\mathrm{s}$ can safely taken to be constant. As Fig. 13b shows, at $x$ we have a tension of strength $T_\mathrm{s}$ as force pointing upward to the left but making an angle $\varphi$ with the $x$-axis whereas at $x + \Delta x$ we have a tension as force of the very same strength as $T_\mathrm{s}$ but pointing downward to the right and making an angle $\varphi + \Delta\varphi$ with the $x$-axis. As we have seen, forces are small, and accordingly angles are small too. Accordingly, the resulting force in vertical direction equals $T\Delta\varphi$ whereas the one in horizontal direction is $\mathscr{O}\{(\Delta\varphi)^2\}$ and, hence, is negligible as $\Delta\varphi \to 0$.

We also know $\tan\varphi = \partial_x w$ so that, for small angles, $\varphi = \tan\varphi = \partial_x w$ and $\Delta\varphi = (\partial_x\varphi)\Delta x = (\partial_x^2 w)\Delta x$. Using Newton's law

we then find, as the $\Delta x$ cancel on the left and on the right,

$$\rho\partial_t^2 w - T\partial_x^2 w = 0\,. \tag{49}$$

Generalizing to a homogeneous membrane in two dimensions we arrive at $w = w(x, y; t)$ obeying

$$(\rho / T)\,\partial_t^2 w - \Delta w = 0 \tag{50}$$

where $\Delta = \partial_x^2 + \partial_y^2$ is the two-dimensional Laplace operator. Keeping an eye on Newton's law, one may add an external force density $f$ to the right-hand side as source term. We clearly see that the tension $T$, and not the bending, is the driving force of the eardrum's motion, as befits a drum. Moreover, the dynamics of (50) is governed by $\Delta$ and not by its square $\Delta^2$ as in (48).

Finally, and most importantly, we focus on the boundary conditions. The tympanum is the gate between the sound outside and the auditory sensory processing inside the auditory cavity connecting the two eardrums. In the case of the monitor lizard of Fig. 1a and in fact of any eardrum in nature, the amplitudes are maximally 40 nm so that locally, say, sampled on a region of 1 mm diameter, the eardrum is flat. Only the extracolumella breaks the rotational symmetry and induces tension. Despite the globally present curvature, one can model this eardrum to high accuracy (Vedurmudi et al., 2016a, Eqs. 1–12) as a sectorial flat membrane rigidly clamped between angles $\phi = \pm\beta$, meaning that its vibrating part is limited to a circular sector between $\beta < \phi < 2\pi - \beta$ with vanishing amplitudes between $\phi = \pm\beta$. The present and final argument underlines the universality of the ICE model (Vedurmudi et al., 2016a, b).

## References


Beranek, L.L., 1986. Acoustics. Electrical and Electronic Engineering. American Institute of Physics.

Christensen-Dalsgaard, J., Manley, G.A., 2005. Directionality of the lizard ear. J. Exp. Biol. 208, 1209–1217.

Christensen-Dalsgaard, J., Manley, G.A., 2008. Acoustical coupling of lizard eardrums. J. Assoc. Res. Otolaryngol. 9, 407–416.

Funnell, W.R.J., Laszlo, C.A., 1978. Modeling of the cat eardrum as a thin shell using the finite-element method. J. Acoust. Soc. Am. 63, 1461–1467.

Han, D., Young, B.A., 2016. Anatomical basis of dynamic modulation of tympanic tension in the water monitor lizard, *Varanus salvator*. Anat. Rec. 299, 1270–1280.

Han, D., Young, B.A., 2018. Biophysical heterogeneity in the tympanic membrane of the asian water monitor lizard, *Varanus salvator*. Zoomorphology 137, 337–348.

Heider, D., van Hemmen, J.L., 2019. Geometric perturbation theory and acoustic boundary condition dynamics arXiv:1912.11008.

Helfrich, W., 1973. Elastic properties of lipid bilayers. Z. Naturforschung C 28, 693–703.

van Hemmen, J.L., Christensen-Dalsgaard, J., Carr, C.E., Narins, P.M., 2016. Animals and ICE: meaning, origin, and diversity. Biol. Cybern. 110, 237–246.

van Hemmen, J.L., Leibold, C., 2007. Elementary excitations of biomembranes: differential geometry of undulations in elastic surfaces. Phys. Rep. 444, 51–99.

Irving, R.S., 2004. Integers, Polynomials, and Rings. Springer-Verlag, New York.

Johnson, M.W., Reissner, E., 1958. On transverse vibrations of shallow spherical shells. Q. Appl. Math. 15, 367–380.

Kreyszig, E., 2010. Advanced Engineering Mathematics. John Wiley & Sons.

Manley, G.A., 1990. Peripheral Hearing Mechanisms in Reptiles and Birds. Springer Berlin Heidelberg.

Marx, S., Schilling, J., Sackmann, E., Bruinsma, R., 2002. Helfrich repulsion and dynamical phase separation of multicomponent lipid bilayers. Phys. Rev. Lett. 88, 138102.

Michelsen, A., Larsen, O.N., 2008. Pressure difference receiving ears. Bioinspiration Biomim. 3, 011001.

Murphy, J.B., Lamoreaux, W.E., 1978. Threatening behavior in mertens' water monitor *Varanus mertensi* (sauria: varanidae). Herpetologica 34, 202–205.

Murphy, J.B., Mitchell, L.A., 1974. Ritualized combat behavior of the pygmy mulga monitor lizard, *Varanus gilleni* (sauria: varanidae). Herpetologica 30, 90–97.

Owerkowicz, T., Carrier, D., Brainerd E, L., 2001. Electromyographic pattern of the gular pump in monitor lizards. Bull. Mus. Comp. Zool. 156, 237–248.

Owerkowicz, T., Farmer, C.G., Hicks, J.W., Brainerd, E.L., 1999. Contribution of gular pumping to lung ventilation in monitor lizards. Science 284, 1661–1663.

Reissner, E., 1955. On transverse vibrations of thin, shallow elastic shells. Q. Appl. Math. 13, 169–176.

Reissner, E., 1996. Selected Works in Applied Mechanics and Mathematics. Jones & Bartlett, Burlington, MA.

Schomburg, W.K., 2015. Introduction to Microsystem Design. Springer-Verlag Berlin Heidelberg.

Timoshenko, S., Woinowsky-Krieger, S., 1959. Theory of Plates and Shells. McGraw-Hill Book Company, New York.

Vedurmudi, A.P., Christensen-Dalsgaard, J., van Hemmen, J.L., 2018. Modeling underwater hearing and sound localization in the frog *Xenopus laevis*. J. Acoust. Soc. Am. 144, 3010–3021.

Vedurmudi, A.P., Goulet, J., Christensen-Dalsgaard, J., Young, B.A., Williams, R., van Hemmen, J.L., 2016a. How internally coupled ears generate temporal and amplitude cues for sound localization. Phys. Rev. Lett. 116, 028101.

Vedurmudi, A.P., Young, B.A., van Hemmen, J.L., 2016b. Internally coupled ears: mathematical structures and mechanisms underlying ICE. Biol. Cybern. 110, 359–382.

Vossen, C., Christensen-Dalsgaard, J., van Hemmen, J.L., 2010. Analytical model of internally coupled ears. J. Acoust. Soc. Am. 128, 909–918.

Wever, E.G., 1978. The Reptile Ear: its Structure and Function. Princeton University Press, Princeton, NJ.

Young, B.A., 2016. Anatomical influences on internally coupled ears in reptiles. Biol. Cybern. 110, 255–261.